

Supporting information for:
**Continuous size-based DEP separation of particles using bi-gap
electrode pair**

Reza Derakhshan,^a Abas Ramiar,^{*,b} Amirhosein Ghasemi^c

^a PhD Student, Mechanical Engineering Department, Microfluidics and MEMS lab, Babol Noshirvani University of Technology, Babol, Iran

^b Associate professor, Faculty of Mechanical Engineering, Microfluidics and MEMS lab, Babol Noshirvani University of Technology, Tel/Fax: +981132334205, Postal Code: 4714873113.

^c PhD, Mechanical Engineering Department, Microfluidics and MEMS lab, Babol Noshirvani University of Technology, Babol, Iran

*: Corresponding author

Email: aramiar@nit.ac.ir

Table of contents:

Fig. S1	S2
Fig. S2	S3
Table S1	S3
Fig. S3	S4
Sec. S1: Comparison between experimental and numerical results	S4
Fig. S4	S6
Fig. S5	S6

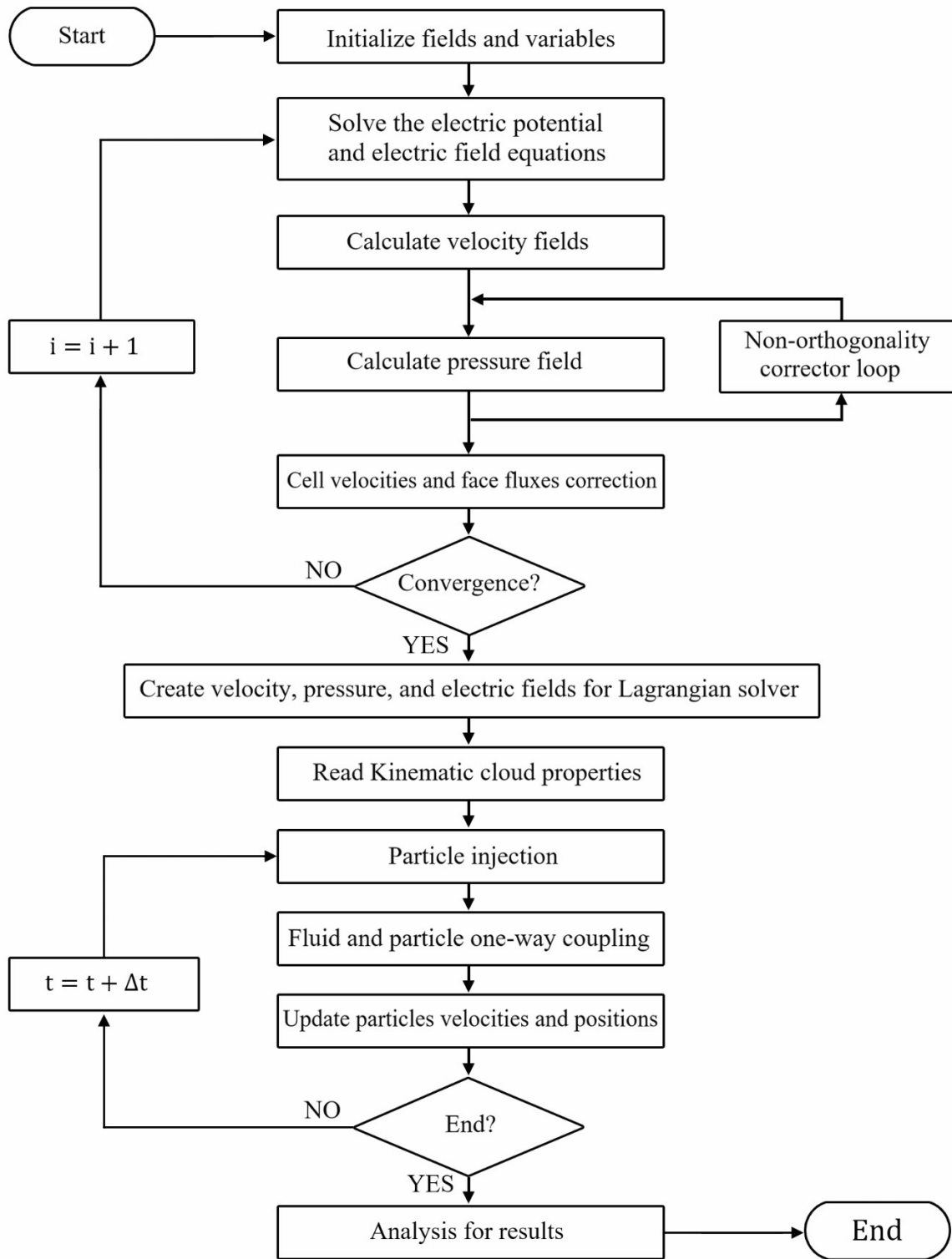


Fig. S1: Flowchart of numerical simulation

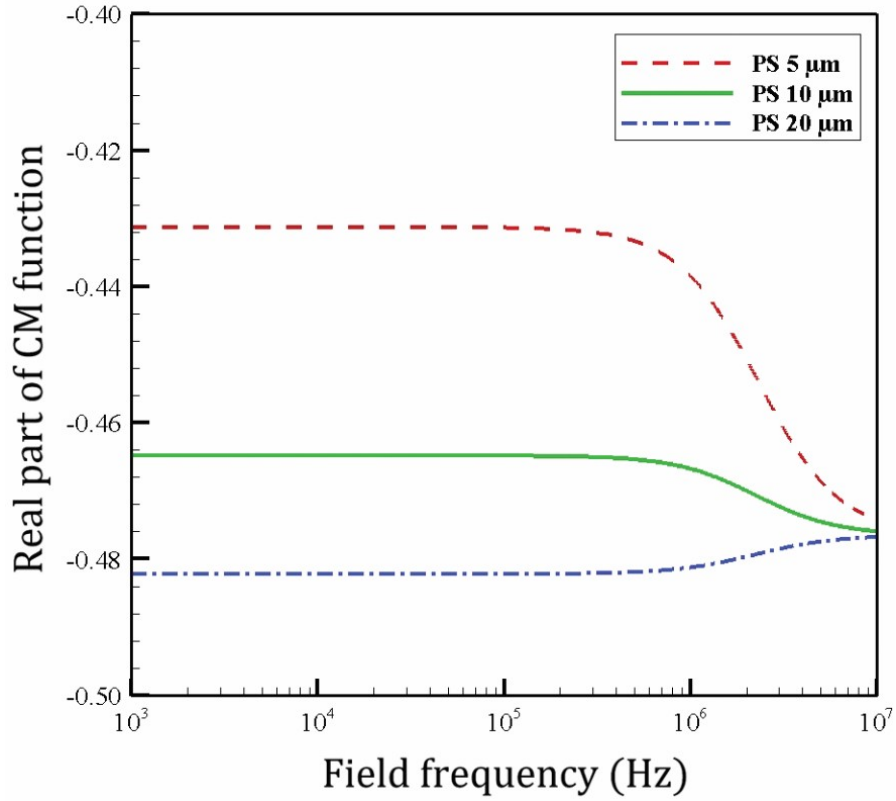


Fig. S2: The real part of Clausius-Mossotti (CM) factor of 5, 10 and 20 μm polystyrene particles ($\sigma_m = 0.01\text{S/m}$).

Table S1: Material properties of solution and particles.

Symbol	Description	Value
σ_m	Electrical conductivity of fluid	0.01 (S/m)
ε_m	Permittivity of fluid	$80.2 \varepsilon_0$
ε_0	Vacuum permittivity	8.85×10^{-12} (F/m)
f	Frequency	100 (kHz)
ρ_m	Density of fluid	1000 (kg m^{-3})
η	Viscosity of fluid	10^{-3} ($\text{kg m}^{-1} \text{s}^{-1}$)
K_s	Surface conductance of polystyrene	1.2 (nS)
ε_p	Permittivity of polystyrene	$2.55 \varepsilon_0$

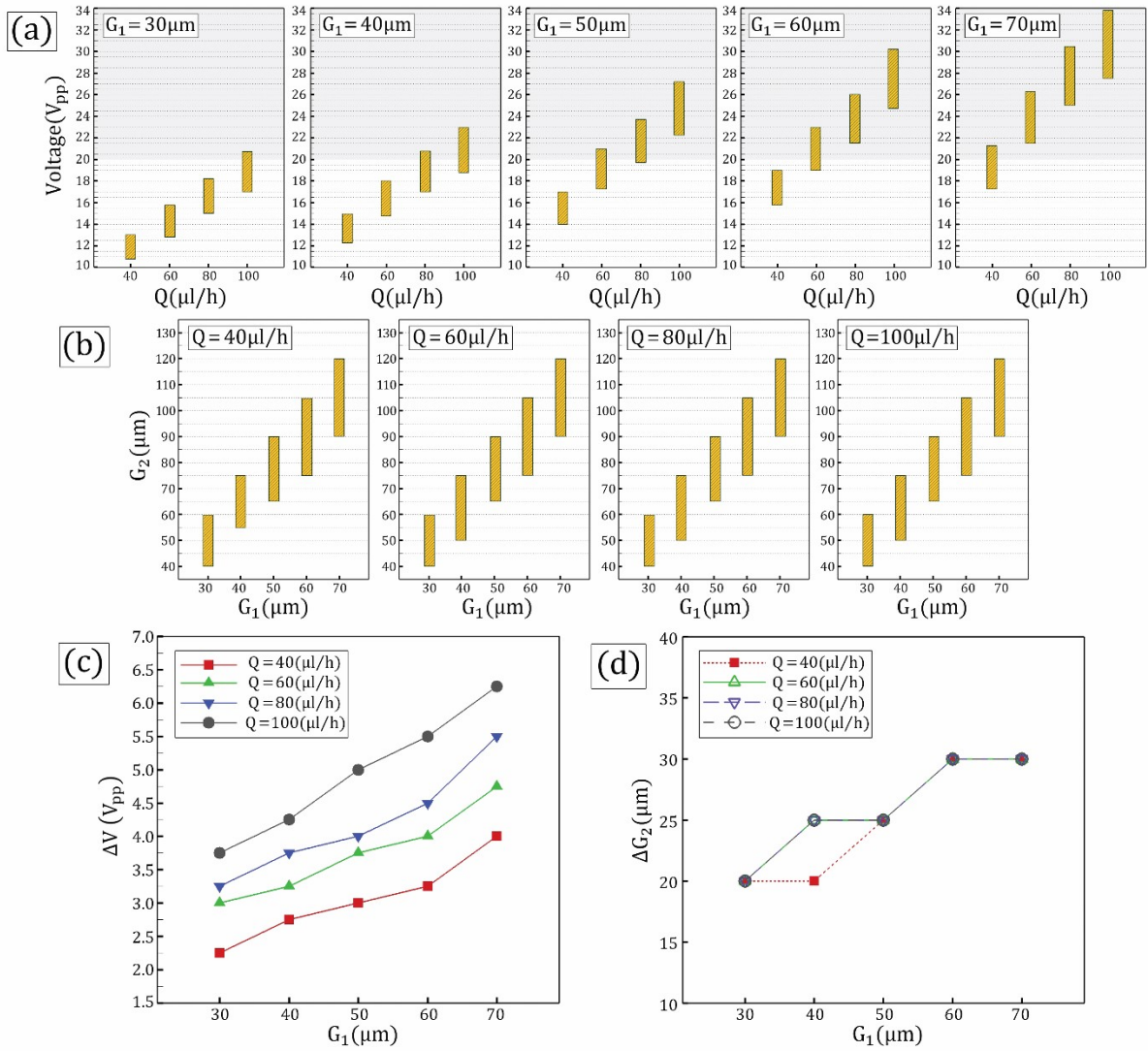


Fig. S3: (a) The suitable voltage window for separating 5 μm particles from larger particles (10 μm), (b) the large gap window, (c) the difference between the upper and lower limits of the voltage window, and (d) the difference between the upper and lower limits of the large gap window for different values of flow rates and small gaps of the electrode pair, at the electrode angle of 30° .

Sec. S1: Comparison between experimental and numerical results

In the first part of the experimental tests, the paths of 5, 10, and 20 μm polystyrene particles are investigated under the influence of DEP force at different flow rates, and the results are compared with numerical simulations. To do this, three samples containing 5, 10, and 20 μm particles are prepared separately. In all experiments, the desired sample and sheath flow are injected into the device from the designated inlets with a flow rate ratio of 1 to 4. A 16 V_{pp} sinusoidal electric potential with a frequency of 100 kHz is applied to only one electrode pair of configuration B. After entering the main channel, the sample flow is concentrated in a

narrow region by the sheath flow. After reaching the active electrode pair, the concentrated particles can be deflected up to a certain distance by the nDEP force in the lateral direction of the channel, depending on the flow rate and their size. To evaluate the particle deflection, in each experiment, the paths of all particles were tracked and recorded in a specific area near the end of the main channel. Fig. S4 shows experimental and numerical simulation results of the particle populations percentage passing over different positions of the channel width at three flow rates of 40 $\mu\text{l/h}$, 60 $\mu\text{l/h}$, and 80 $\mu\text{l/h}$. In a constant voltage, with increasing flow rate and consequently increasing the drag force on the particles, the amount of lateral displacement of all particles decreases. By comparing the experimental tests and numerical simulations results, it can be claimed that the newly developed solver has very high accuracy, and its results agree well with experimental tests. To have a better understanding of how different particles move under the influence of DEP force in the channel, the image of particles passing over an active electrode pair (configuration B) at a flow rate of 60 $\mu\text{l/h}$ is shown in Fig. S5. As shown in Fig. S5a, it is clear that 5 μm polystyrene particles, which are experiencing a weak nDEP force due to their smaller size, pass over the electrode pair without significant deviation and continue their way toward the desired outlet. The produced DEP force decreases with a sudden increase in the electrode pair gap (from $G_1 = 40 \mu\text{m}$ to $G_2 = 65 \mu\text{m}$). Therefore, after a sudden increase in the electrode pair gap, the DEP force decreases, which causes the 10 μm particles to move towards the outlet under the influence of drag force and stop moving along the electrode pair length, which can be seen in Fig. S5b. On the other hand, 20 μm polystyrene particles continue to experience strong DEP force due to their larger size and deflect to the lateral direction of the channel up to the end of the electrode pair length. A closer look at Fig. S5c shows that 20 μm polystyrene particles move at a considerable distance from the edge of the first electrode in areas where the electrode pair has a gap of G_1 . After reaching the larger gap (the areas where the electrode pair has a G_2 gap), they move closer to the edge of the first electrode. This indicates a reduction in the DEP force. On the other hand, 10 μm particles, unlike 20 μm particles, move very close to the edge of the first electrode pair in areas where the electrode pair has a G_1 gap. This is another clear reason to claim that 10 μm particles experience a weaker DEP force than 20 μm particles.

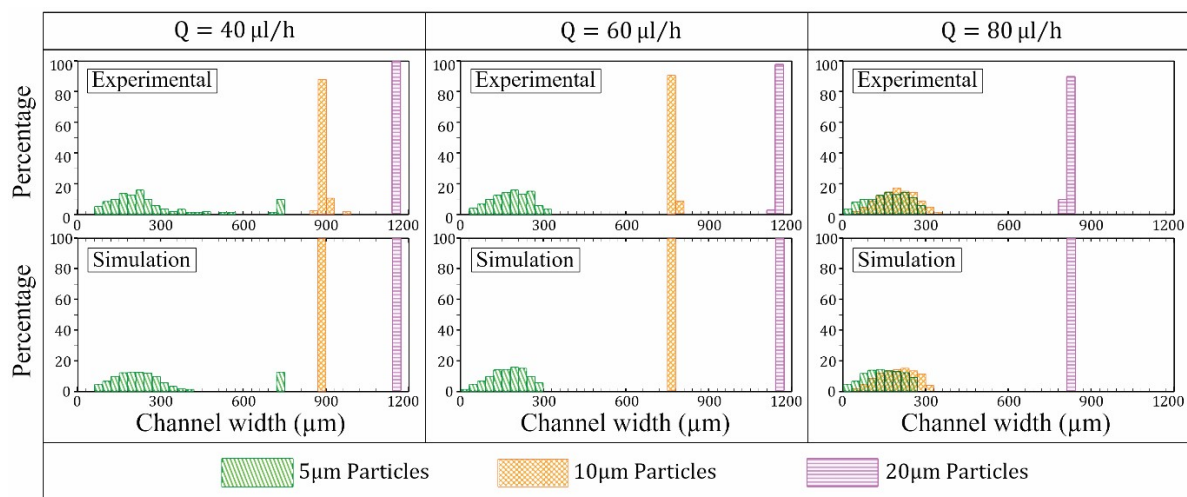


Fig. S4: Experimental and numerical simulation results of the percentage of 5, 10, and 20 μm particle populations passing over different positions of the channel width at three flow rates of 40 $\mu\text{l/h}$, 60 $\mu\text{l/h}$, and 80 $\mu\text{l/h}$, when a 16 Vpp sinusoidal electric potential with a frequency of 100 kHz is applied to a pair of electrode configuration B.

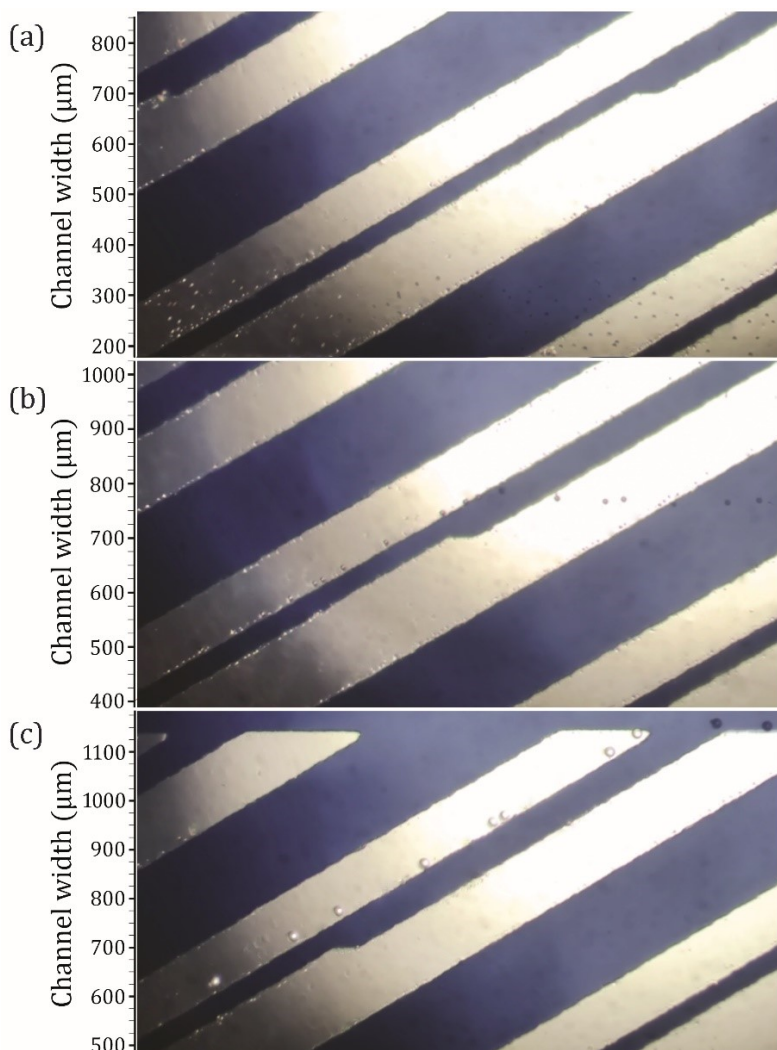


Fig. S5: The image of passing (a) 5 μm polystyrene particles, (b) 10 μm polystyrene particles, and (c) 20 μm polystyrene particles over an active electrode pair of configuration B at a flow rate of 60 $\mu\text{l/h}$ and a 16 Vpp sinusoidal electric potential applied with a frequency of 100 KHz.